Geomechanics and Engineering, *Vol. 29, No. 3 (2022) 359-368*
https://doi.org/10.12989/gae.2022.29.3.359

Evaluation of rock cutting efficiency of the actuated undercutting mechanism

Hoyoung Jeong[**1a], Yudhidya Wicaksana[**2b], Sehun Kim[3c] and Seokwon Jeon[*3]

[1]*Department of Energy Resources Engineering, Pukyong National University, 45 Yongso-ro Nam-gu Busan 48513, Republic of Korea*
[2]*Center for Industrial Engineering, Institut Teknologi Bandung, Jalan Ganesha 10 Coblong Bandung 40132, Indonesia*
[3]*Department of Energy Resources Engineering, Research Institute of Energy and Resources, Seoul National University, 1 Gwanak-ro Gwanak-gu Seoul 08826, Republic of Korea*

(Received December 15, 2021, Revised February 17, 2022, Accepted March 5, 2022)

Abstract. Undercutting using an actuated disc cutter (ADC) involves more complex cutting mechanism than traditional rock cutting does, requiring the application of various new cutting parameters, such as eccentricity, cutter inclination angle, and axis rotational speed. This study presents cutting-edge laboratory-scale testing equipment that allows performing ADC tests. ADC tests were carried out on a concrete block with a specified strength of 20 MPa, using a variety of cutting settings that included penetration depth (p), eccentricity (e), and linear velocity (v). ADC, unlike pick and disc cutting, has a non-linear cutting path with a dynamic cutting direction, requiring the development of a new method for predicting cutting force and specific energy. The influence of cutting parameters to the cutter forces were discussed. The ratio of eccentricity to the penetration depth (e/p) was proposed to evaluate the optimal cutting condition. Specific energy varies with e/p ratio, and exhibits optimum values in particular cases. In general, actuated undercutting may potentially give a more efficient cutting than conventional pick and disc cutting by demonstrating reasonably lower specific energy in a comparable cutting environment.

Keywords: actuated disc cutter; rock cutting performance; specific energy; undercutting mechanism

1. Introduction

Mechanical cutting studies have mostly focused on two types of cutting (e.g., roller disc cutting and drag pick cutting) and cutting characteristic of them (Cho *et al.* 2013, Jeong *et al.* 2016, Chang *et al.* 2017, Copur *et al.* 2017, Zhu *et al.* 2017, Jeong and Jeon 2018, Zhang *et al*. 2020). They have differences in the direction of cutting motion of the tools relative to the rock surface: a drag cutter moves across the rock surface at a certain penetration depth, directly causing development of tensile cracks; in contrast, an indenting cutter such as a disc cutter, is penetrating perpendicular to the rock surface, causing first the formation of a crushed zone beneath the tool and consequently the creation of secondary tensile crack (Dehkhoda and Detournay 2017). Both types of cutting tool have their pros and cons. Roller disc cutting needs a high thrust force to induce tensile failure, but the mechanism allows the contact zone between rock and tool to change during the process, reducing thermal stress-induced wear (Hood and Alehossein 2000). On the other hand, drag pick cutting requires less energy than disc cutting because the tensile failures are generated more directly. However, the dragging mechanism is prone to wear due to constant contact of the same area of the tool throughout the procedure (Hood and Roxborough 1992).

Rock cutting using an undercutting disc cutter (UDC) has been proposed as an alternative method that benefits both rolling and dragging mechanism. The undercutting concept allows a rolling disc to be dragged across the rock surface like a pick cutter. Because tensile fractures are formed directly, and thermal wear is dispersed due to the rotational movement of the disc, the combination of these two principles results in an efficient cutting. Hood and Alehossein (2000) emphasized the significance of this principle, which permits a hard rock to be excavated efficiently without causing excessive wear of a cutter. The principle is implemented in certain types of mining machinery, such as Wirth's Continuous Mining Machine and Tunnel Boring Extender (Ramezanzadeh and Hood 2010).

Recently, the UDC technique has been advanced to undercutting with oscillated disc cutter (ODC) and actuated disc cutter (ADC), in which the disc can oscillate at small amplitudes with the aid of an internal motor. The analytical model of ODC was well described in previous study (Kovalyshen 2015). ADC adopts the characteristics of an ODC with the addition of a free rotational mechanism in a second axis that is not concentric with the main motored-rotational axis. The ADC mechanism enables easy adjustment of the oscillation amplitude and frequency of the rotation via its secondary axis (Karekal 2013, Dehkhoda and Detournay 2017, 2018, 2019, Dehkhoda and Hill 2019, Xu and Dehkhoda 2019, Xu *et al.* 2021).

This paper analyzed the results based on the undercutting test using ADC performed by a state-of-the-art

∗Corresponding author, Professor
E-mail: sjeon@snu.ac.kr
**These authors contributed equally to this work
[a]Assistant Professor
[b]Research Assistant Professor
[c]Undergraduate Student

ISSN: 2005-307X (Print), 2092-6219 (Online)

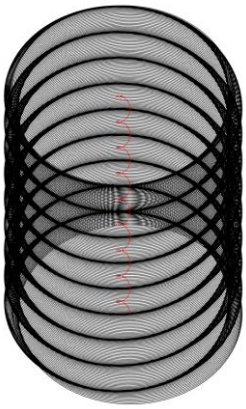

(a) v=20 mm/s, e=3.75 mm, RPM=70

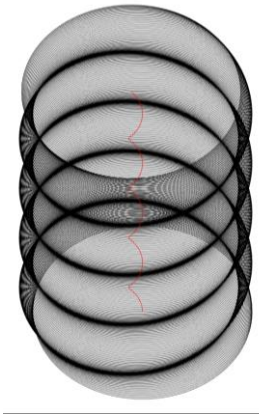

(b) v=40 mm/s, e=3.75 mm, RPM=70

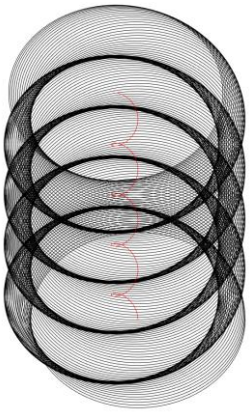

(c) v=40 mm/s, e=7.5 mm, RPM=70

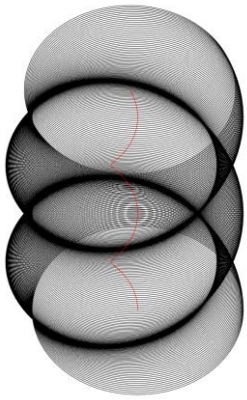

(d) v=40 mm/s, e=7.5 mm, RPM=35

Fig. 1 Cutting trajectories of ADC with different cutting parameters (red line represents the path of disc center)

undercutting test rig. We performed tests with various parameters including penetration depth, actuation amplitude (eccentricity), and linear velocity. Additionally, we developed a new method for calculating the specific energy of ADC cutting, which differs from the one used in the traditional disc and pick cutting.

2. Experimental method

2.1 ADC Mechanism

A thorough assessment of the mechanics of actuated undercutting has been introduced in Dehkhoda and Detournay (2017, 2019) and Jeong *et al*. (2020b, 2021). The mechanism of the actuated undercutting system is unique in that it involves two axes of rotation. The main axis is where the system rotates, whereas the secondary axis is the center of the disc, which can be modified off-centric to the main axis. Eccentricity (e) is defined as the distance between the two axes. The system revolves at a constant angular velocity (ω) around the primary axis. Hereafter, the angular

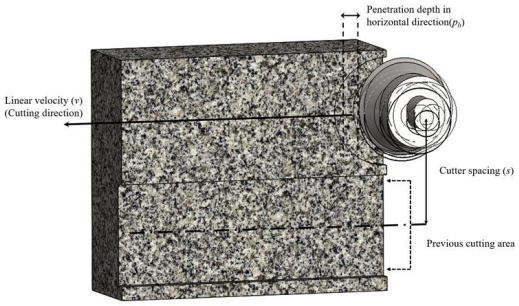

(a) Top view

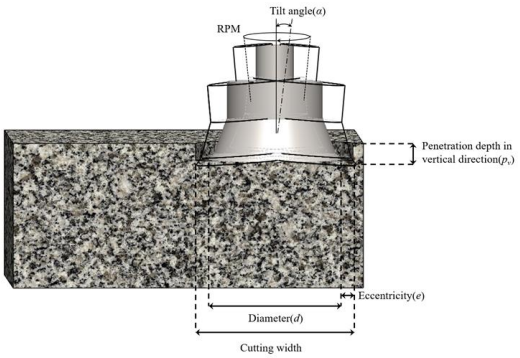

(b) Front view

Fig. 2 Cutting parameters of undercutting using an actuated disc cutter

velocity ω is expressed as the term "RPM" because the angular velocity can be easily converted to RPM, which can be set with the testing system introduced in Section 2.2. The undercutting disc is attached to a cartridge and moves with a constant linear velocity (v) parallel to the cutting direction. The movement of a disc is determined by the product of translation and actuation relative to the main axis. For example, as illustrated in Fig. 1, the movement of ADC was significantly affected by the linear velocity, RPM, and eccentricity.

The disc rotates freely around its axis, cutting the rock surface at a constant vertical penetration depth (p_v); hereafter, the p_v was expressed as the p to keep the original definition of penetration depth (or depth of cut), while penetration depth in horizontal direction was expressed as p_h which is a function of linear velocity and rotation speed (See Fig. 2(a)). The operation will produce a cut volume with a consistent depth and width. The parameters e, RPM, v, p, and the diameter of the undercutting disc (d) define the geometry of the cut rock surface. Additionally, the disc can be tilted (tilt angle α) throughout the cutting process to avoid excessive friction on the flat surface of the disc. The schematic mechanism can be seen in Fig. 2.

2.2 ADC testing system

The actuated undercutting test system used in this study is shown in Fig. 3(a). Fig. 3(b) shows a picture of the cutting tool and specimen for the ADC cutting test. The machine consists of a rigid platform, electric motors, a three-dimensional load cell, a mounting system for the

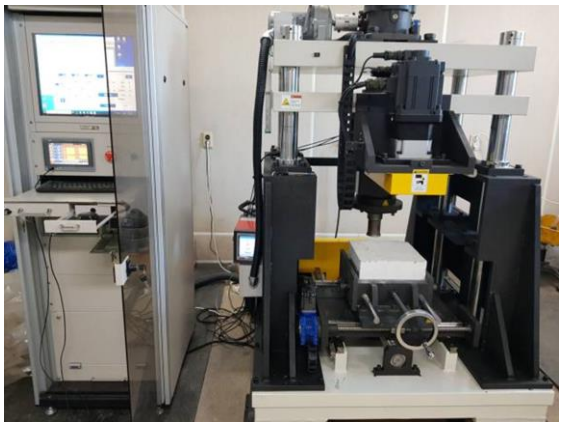

(a) Overview

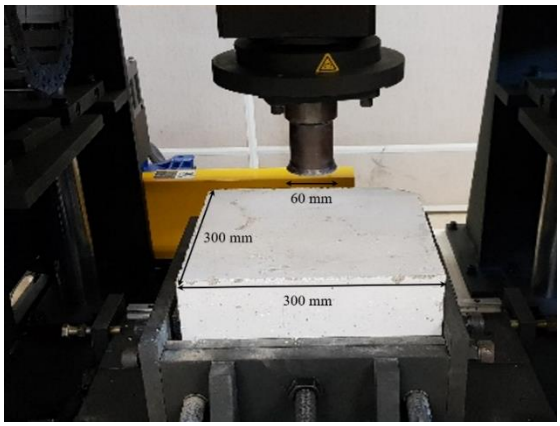

(b) Cutting tool and specimen

Fig. 3 ADC testing system

actuated disc, a rock block container, and a data acquisition system connected to a personal computer. The load cell is capable of recording forces in three orthogonal axes and has a capacity of 20 tons in each direction. The system is equipped with three electric motors. The vertical motor is used to control the penetration depth, while the horizontal motor is used to drive the linear movement at a maximum speed of 100 mm/s. Another electric motor with a maximum RPM of 800 and a torque of 1000 Nm serves as the rotational motor of the system. Most of the settings can be modified via a built-in controller and software, except for eccentricity and tilt angle, which can be adjusted manually.

2.3 Sample preparation

The specimen container can hold a rock block up to 300 mm × 300 mm × 300 mm in size. Given the maximum specimen size, installing the full-size disc from the actual excavation equipment, which is typically 500 to 550 mm in diameter, is incompatible. Therefore, the scaled-down disc cutter shall be used, and the effect on the scale should be considered. As shown in Fig. 4, the scaled-down ADCs are available in various sizes in the laboratory, ranging from 60 to 150 mm in diameter. Fig. 5 shows a schematic drawing of ADC of 60 mm in diameter. The scaling ratio is calculated through dimensional analysis. For instance, as shown in Table 1, we used a 60 mmϕ ADC in the laboratory

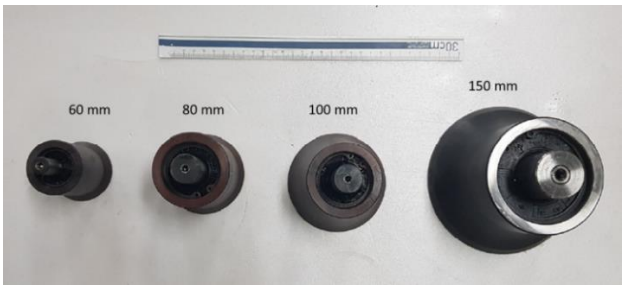

Fig. 4 Scaled-down ADCs in various sizes

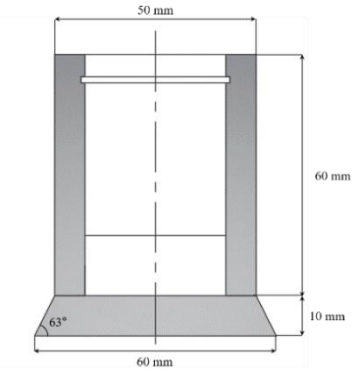

Fig. 5 A schematic drawing of an ADC of 60 mm in diameter

Table 1 Scaled condition used in the experiment (ADC diameter = 60 mm, specimen density = 2.1 g/cm^3)

Variables	Dimension	Measure		Ratio
		Scaled	Actual	
Length	L	60	500	0.120
Gravity	LT^{-2}	9.81	9.81	1.000
Density	ML^{-3}	2.1	2.6	0.808
Time	T	-		0.346
Mass	M	-		0.001
Strength and stress	$ML^{-1}T^{-2}$	-		0.097

Table 2 Mechanical properties of concrete specimen used in this study

Properties	Unit	Value
Dry density	g/cm^3	2.1
Uniaxial compressive strength	MPa	20.2
Brazilian tensile strength	MPa	2.12
Young's Modulus	GPa	15.27
Poisson's ratio		0.08
Porosity	%	13.41
Maximum size of coarse aggregate	mm	25

to cut a concrete block of about 20 MPa in uniaxial compressive strength and of 2.1 g/cm^3 in density. In actual operation, we presume to use a 500 mmϕ ADC to cut a rock with a density of 2.6 g/cm^3. Assuming that the gravitational acceleration is constant, the ratio of the rest of the dimensional variables can be derived. Based on the

dimensional analysis, it can be inferred that the strength of the material tested in the laboratory is reduced 10.3 times from the actual condition (1/0.097 = 10.3). In other words, the 20 MPa strong specimen in the laboratory experiment is equivalent to about 206 MPa in the actual cutting operation. The mechanical properties of the concrete are summarized in Table 2.

2.4 Specific energy calculation

The concept of specific energy is introduced to evaluate the rock cutting performance, and it has been used to estimate the performance of mechanical excavators (Kim *et al.* 2020). The term specific energy refers to the work performed by a cutter to cut a unit volume of rock, as shown in Eq. (1).

The cutting direction is linear for disc and pick cutting, and the force can be represented by force dominant parallel to the cutting direction. Thus, the work performed by the cutter on a typical traditional cutting can be calculated using Eq. (2).

$$SE = \frac{Work\ \ done}{Volume} \tag{1}$$

$$W = \overrightarrow{F_c} \cdot \vec{l} = |\overrightarrow{F_c}||\vec{l}|cos\theta \tag{2}$$

where F_c is the cutting (or rolling) force, l is the cutting length, and θ is the angle between the force direction and the cutting direction; θ is zero degree in case of the disc and pick cutting.

However, in actuated undercutting, the cutting force and side force play a significant role in the cutting operation. As a result, work is derived in a slightly more complex form by including side force. The DAQ system of the machine is capable of recording three-dimensional force at the rate of 1000 Hz. The quick data interval enables segmentation of the cutting trajectory into smaller linear segments every one millisecond. As a result, the work is denoted by Eq. (3), where F_c is the cutting force, F_s is the side force, and dl is the cutting length in small time interval. The force direction was determined by the direction cosine of resultant force vector while the cutting direction was calculated by direction cosine of displacement vector which can be determined by adjacent locations of an ADC; thus, the angle θ was defined by those two directions. Also, it is noted that "*dl*" is a calculated discrete value from the measured data rather than a derivative term (in terms of mathematical expression) respected to infinitesimal time.

The cut volume is simplified and assumed to be cuboid in shape because the excavation produces a flat surface with straight side boundaries. Thus, as illustrated in Eq. (4), the cutting volume is theoretically estimated.

$$W = \sum(|\overrightarrow{F_c} + \overrightarrow{F_s}| \cdot dl \cdot cos\theta) \tag{3}$$

$$V_{cut} = (d + 2e)pl \tag{4}$$

where d is the diameter of the cutter, e is the eccentricity, p is the penetration depth, and l is the cutting length.

Considering the work and volume calculations explained above, the specific energy can be denoted as Eq. (5). The schematic description of the calculation is depicted in Fig. 6.

$$SE = \frac{1}{V_{cut}} \sum(|\overrightarrow{F_c} + \overrightarrow{F_s}| \cdot dl \cdot cos\theta) \tag{5}$$

Otherwise, the specific energy of ADC can be calculated by Eq. (6) (Dehkohda and Detournay 2019).

$$SE = \frac{P}{vdpA} \tag{6}$$

where P is known as average external power, A is the ratio of the average width of the cut over the diameter of the disc (for example, for drag bit A=1), d is cutter diameter, v is the advanced velocity, and p is the penetration depth. The work done by ADC is determined by the directly measured power, which means work per unit time. However, it should be noted here that the external power should be directly measured from an additional measuring device during rock cutting.

3. Result and analysis

This study used the ADC of 60 mm diameter and constant RPM of 70. A total of 15 cases were performed with various linear velocities (v) of 20 mm/s, 30 mm/s, and 40 mm/s, penetration depths (p) of 3 mm, 4 mm, and 5 mm, and eccentricity (e) of 3.75 mm, 5.60 mm, and 7.50 mm. Cutter force was recorded throughout each test in three orthogonal directions (fixed axis in Cartesian coordinate system), namely cutting, side, and normal forces. The specific energy for each case was calculated based on Eq. (5). It is noted that the scale factor was not considered in calculation of cutter forces and specific energy.

3.1 Cutter forces of ADC

The cutter forces are summarized in Table 3. Fig. 7 shows an example of representative cutter forces acting on the ADC during the rock cutting test. Three force components were periodic with a certain level of maximum values. Each mean cutter force was measured by averaging all force data during the cutting test, while peak cutter force was obtained from the averaged value of the local maximum points.

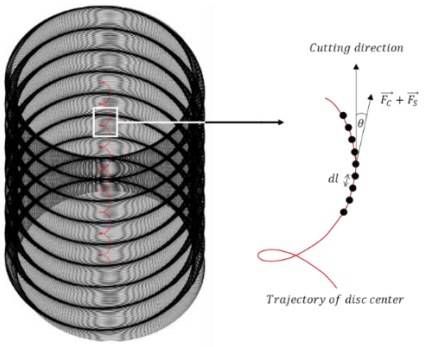

Fig. 6 Sample of cutting trajectory of ADC and specific energy calculation

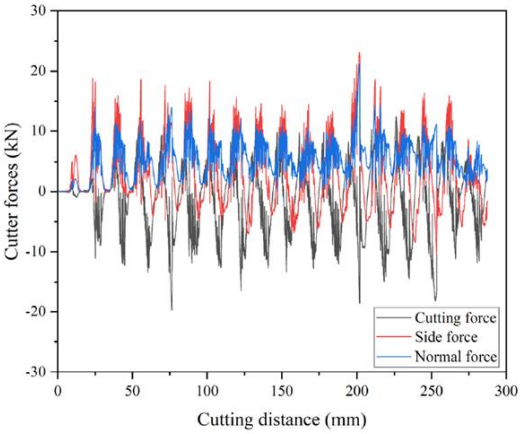

Fig. 7 Representative cutter forces of ADC (d = 60 mm, v = 20 mm/s, p = 3 mm, e = 7.5 mm, RPM = 70)

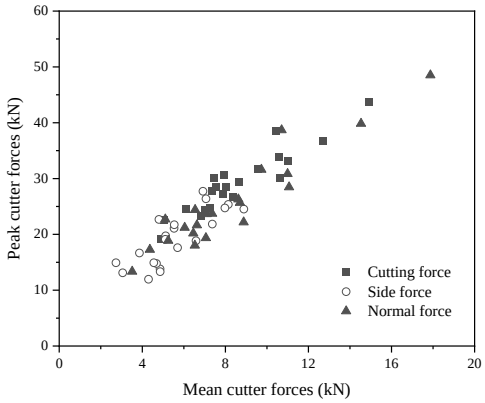

Fig. 8 Relationship between mean and peak cutter forces of an ADC

Fig. 8 shows the relationship between mean cutter forces and peak cutter forces obtained from this study. For all force components, the mean and peak forces are in a significant linear relationship for all cutting conditions. The ratio of peak to mean cutter forces ranged from 2.0 to 3.0 roughly. The values are similar to the range of disc and pick cutters reported in previous studies (Pan *et al*. 2019, Jeong *et al*. 2020c), and as reported by the researchers, it is affected by the roughness of rock surface and brittle characteristics of rock specimen. The strong linear relationship indicates the tendency of changes in mean and peak forces according to the cutting conditions is consistent. Hereafter, the effect of cutting conditions on the cutter force is analyzed in terms of the mean cutter force.

Fig. 9 shows the effect of penetration depth on the cutter force acting on the ADC (only for e = 7.5 mm). As shown in Fig. 9, there is no significant relationship between the penetration depth and cutter force. Overall, all force components seemed to increase with the penetration depth. However, in other cases, the forces decreased or fluctuated with the penetration depth. As the testing data was insufficient, the influence of penetration depth on the cutter force could not be concluded.

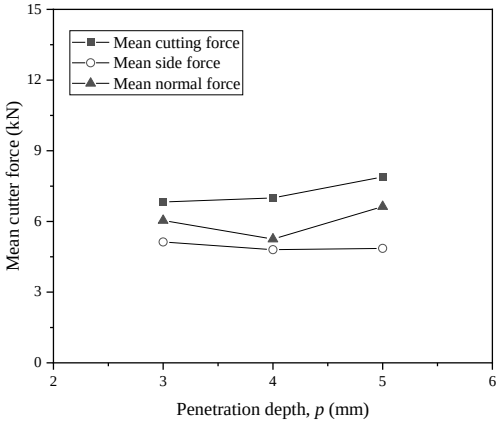

(a) v = 20 mm/s

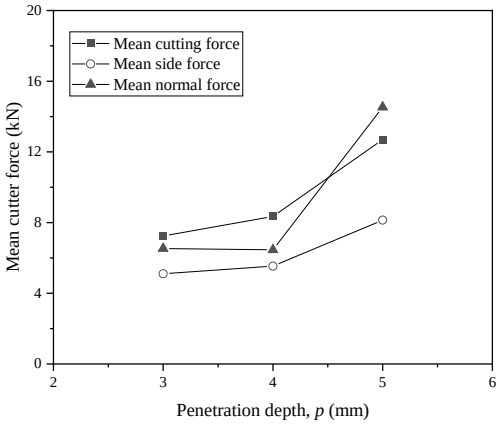

(b) v = 30 mm/s

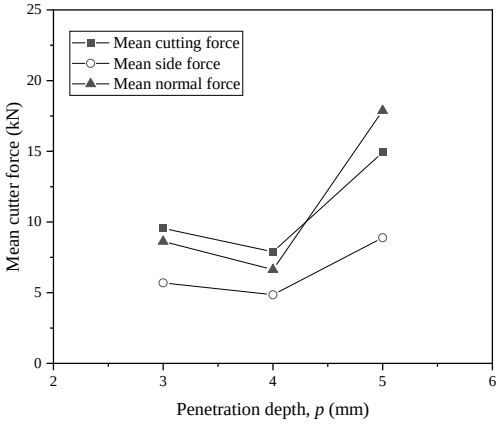

(c) v = 40 mm/s

Fig. 9 Effect of penetration depth on the cutter force of ADC at different linear velocities (e = 7.5 mm)

Fig. 10 shows the effect of linear velocity (v) on the cutter force acting on the ADC. The results indicated that the cutter forces linearly increased with the linear velocity. When the other cutting parameters are constant, linear velocity determines the depth in which the cutter penetrates

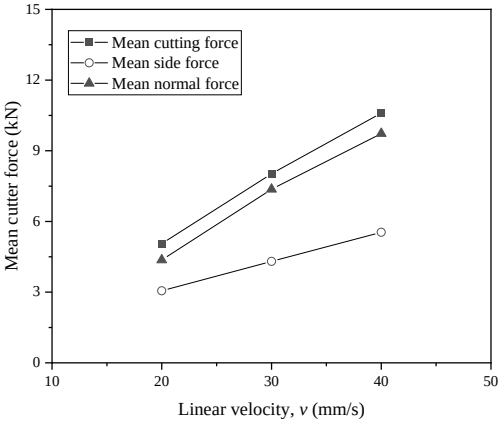

(a) e = 3.75 mm

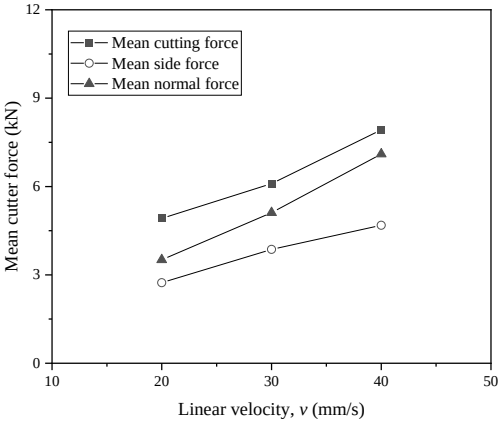

(b) e = 5.6 mm

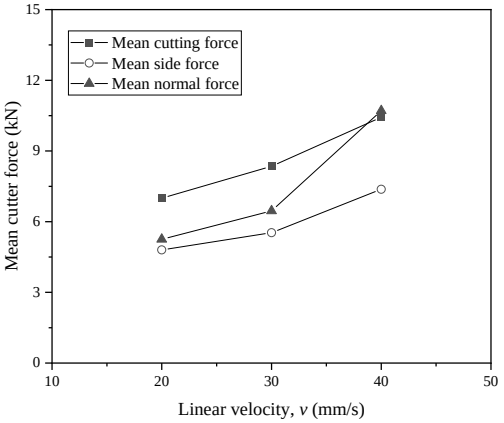

(c) e = 7.5 mm

Fig. 10 Effect of linear velocity on the cutter force of ADC at different eccentricities (p = 4 mm)

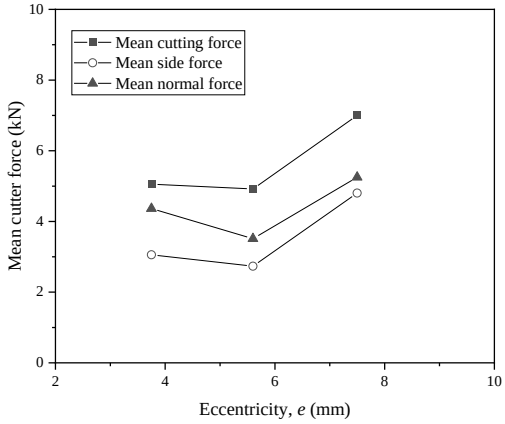

(a) v = 20 mm/s

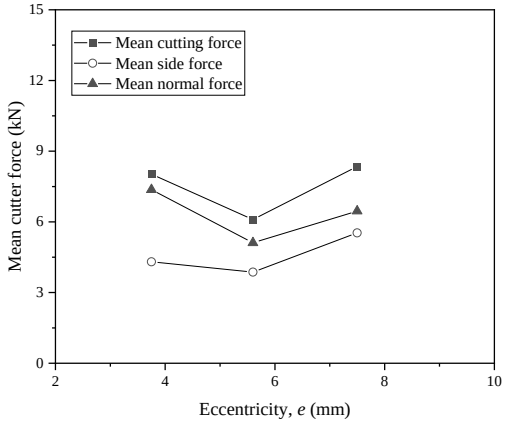

(b) v = 30 mm/s

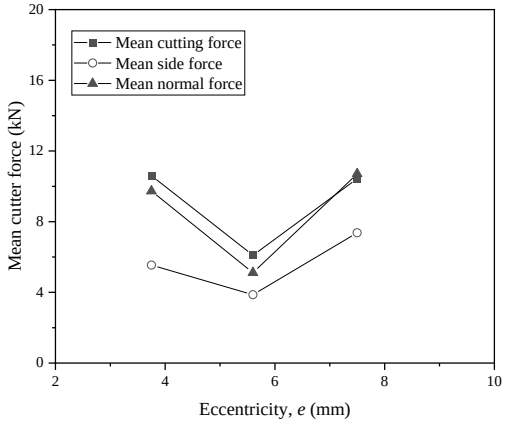

(c) v = 40 mm/s

Fig. 11 Effect of eccentricity on the cutter force of ADC at different eccentricities (p = 4 mm)

(in cutting direction) into the rock per one revolution on the cutting surface. Because the positive (linear or power-function) relationship between the penetration depth and cutter forces has been extensively proven by theoretical, experimental, and numerical research in rock cutting engineering, the results can be thought to be reasonable.

Fig. 11 shows the effect of eccentricity (e) on the cutter forces of the ADC. The results indicated that the cutter

Table 4 Results of specific energy in ADC test

Case	e (mm)	v (mm/s)	p (mm)	Specific energy, SE (MJ/m^3)
1	3.75	20	4	27.67
2	3.75	30	4	47.10
3	3.75	40	4	54.44
4	5.6	20	4	27.03
5	5.6	30	4	33.86
6	5.6	40	4	50.49
7	7.5	20	4	20.51
8	7.5	30	4	51.06
9	7.5	40	4	74.32
10	7.5	20	3	33.69
11	7.5	30	3	44.84
12	7.5	40	3	43.85
13	7.5	20	5	50.45
14	7.5	30	5	84.37
15	7.5	40	5	89.10

*e, v, and p are eccentricity, linear velocity and penetration depth, respectively.

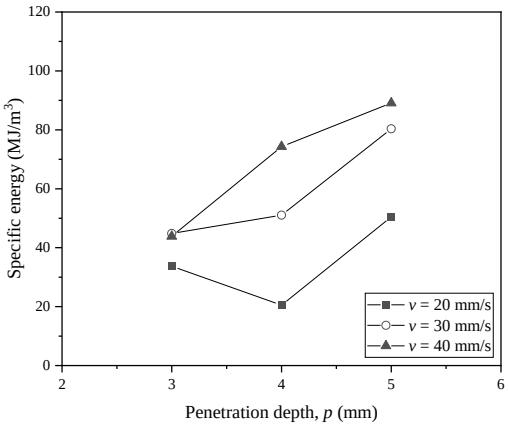

Fig. 12 Effect of penetration depth on specific energy

forces were minimum at 5.6 mm of eccentricity for all cutting conditions. It implies that the cutting efficiency can be optimized at a specific eccentricity value in ADC rock cutting when the other cutting parameter is constant. The cutting efficiency of ADC was discussed in the latter part of this paper (Section 3.2 and 4) in detail.

3.2 Specific energy

The specific energy obtained from ADC cutting tests are summarized in Table 4. In this part, we focused on analyzing the effect of each cutting condition on the specific energy.

Fig. 12 shows the effect of penetration depth (p) on the specific energy of the ADC. At 30 and 40 mm/s of linear velocity, the specific energy increased with the penetration depth. While, at the 20 mm/s, the specific energy had a minimum point at a given penetration depth (4 mm). Based

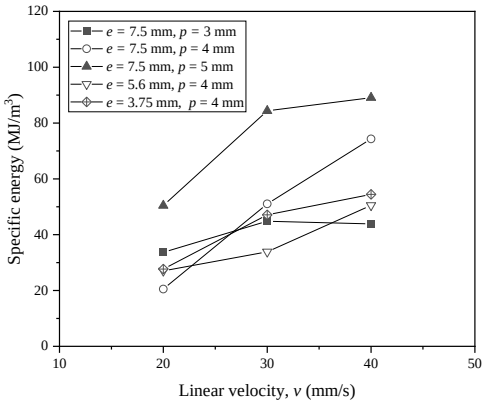

Fig. 13 Effect of linear velocity on specific energy

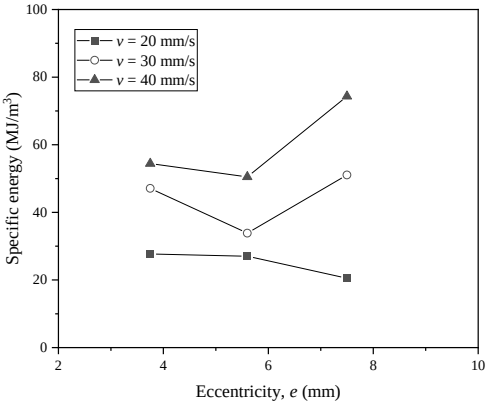

Fig. 14. Effect of eccentricity on specific energy (p = 4 mm)

on the result at the linear velocity of 20 mm/s, it was presumed that the specific energy might be optimized at a certain value of penetration depth. For 30 and 40 mm/s, it was anticipated that the specific energy might be lower at smaller penetration depth; however, it cannot be confirmed due to the lack of available test data. Also, the distinct trend of specific energy according to the linear velocity implies that the optimal value of penetration depth changed with the linear velocity.

Fig. 13 demonstrates the influence of linear velocity (v) on the specific energy. For all cutting conditions, the specific energy tended to rise with the linear velocity. The increase in linear velocity means the increase of horizontal penetration depth when other cutting parameters are constant. Therefore, the linear velocity (or horizontal penetration depth) significantly affects to the cutting efficiency of ADC, and it should be optimized at a given cutting condition. However, it is impossible to define a certain optimal value of linear velocity under considered cutting conditions in this study. It was difficult to conclude the effect of linear velocity on the specific energy within the range of testing data. Further study is required to investigate the effect of linear velocity on the specific energy with extended testing data.

Fig. 14 highlights the effect of eccentricity (e) on the specific energy. At 20 mm/s, the specific energy decreased with the eccentricity. In contrast, the specific energies of 30 and 40 mm/s were minimum at a certain eccentricity (5.6 mm in this study). When the other cutting parameters are constant, the increase of the eccentricity of ADC directly means that ADC cuts a larger volume of rock in rotational motion. These results indicated that the cutting efficiency of ADC increases with the eccentricity until the capability of ADC reaches a certain limit value under the given cutting condition; above a certain eccentricity, the required cutter forces will drastically increase. Consequently, the specific energy can be optimized (or minimized) to a particular cutting condition.

4. Discussion

In traditional disc and pick cutting, the optimum cutting is usually expressed as a function of the *s/p* ratio, the ratio of line spacing between two cutters and penetration depth. Fig. 15 illustrates the influence of line spacing and penetration depth on specific energy and cutting efficiency (Bilgin *et al*. 2014). If the line spacing is too small (case a), the specific energy becomes extremely high, and the cutting becomes inefficient due to the over-crushing of the rock. If the line spacing is too large (case c), the specific energy is also high, and the process is inefficient because the tensile cracks from neighboring cuts cannot connect to form a chip (unrelieved cut). The lowest specific energy is attained by optimizing the *s/p* ratio, as illustrated in case b, which results in the most efficient cutting condition and produces the largest rock chips.

Undercutting with ADC, on the other hand, does not rely on neighboring cuts to produce chips. Fig. 16 shows an example of a cutting surface after the cutting test by ADC. It can be confirmed that there is almost no interaction between the adjacent cutting path, and it agreed with the observation from the previous study (Dehkhoda and Detournay 2017). The ADC enables the generation of tensile cracks in a direct manner, and the tensile cracks propagate directly towards the free surface. In this circumstance, the *s/p* ratio is irrelevant in determining the optimal cutting condition. Furthermore, as explained in Section 3, the results indicated that the force and specific energy of ADC were affected by the various cutting parameters. Also, the relationships between cutting parameters and cutter force and specific energy were not somewhat clear. It means that the use of a combination of cutting parameters (*s/p* ratio in traditional cutting) can be a useful approach to specify the optimum cutting condition in ADC cutting.

We attempt to use the *e*/*p* ratio, which is the eccentricity to penetration depth ratio. Eccentricity is defined as the offset between the disc axis and the main rotational axis. Thus, the unit length of eccentricity contributes to the amount of rock excavated while also affecting the force being used to cut the rock. Therefore, the cutting efficiency will be specified by the minimum *SE* value under various *e/p* ratio settings.

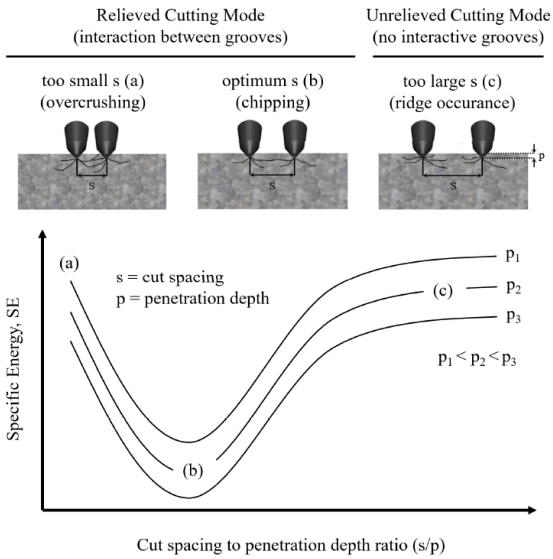

Fig. 15 The influence of line spacing and penetration depth on specific energy and cutting efficiency (modified from Bilgin *et al*. 2014)

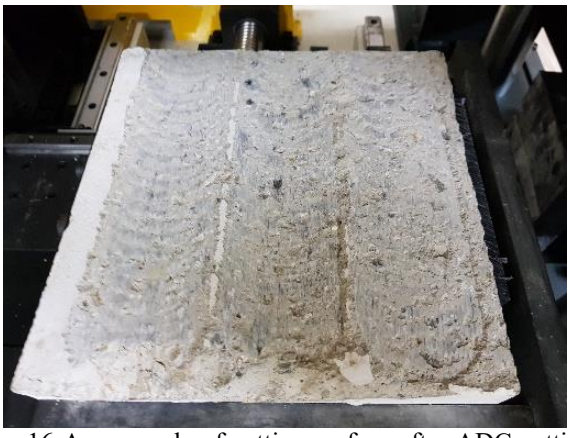

Fig. 16 An example of cutting surface after ADC cutting test

Fig. 17 illustrates the influence of the *e/p* ratio and linear velocity on specific energy. The graph demonstrates that specific energy varies with the *e/p* ratio. At the constant eccentricity (Fig. 17(a)), the specific energy was minimized at *e*/*p* = 1.4; noted that the trend exactly coincides with that shown in Fig. 14 because the eccentricity was fixed as 7.5 mm. In the case of the constant penetration depth (Fig. 17(b)), the specific energy was minimized at 1.875 of *e*/*p* (v = 20 mm/s), while the specific energy continuously decreased with the *e*/*p* at 30 and 40 mm/s of linear velocity. For the latter cases, 30 and 40 mm/s of linear velocity, the optimum *e*/*p* cannot be found due to the limited range of *e*/*p*. Based on the results, it is expected that the *SE* for 30 and 40 mm/s will be minimized at the larger *e*/*p* values. The results indicated the *e*/*p* can be an indicator to define the optimum cutting condition; however, it should be noted that a relatively limited range of testing data within selected cutting parameters are included in this study. Based on these findings, it is anticipated that cutting efficiency should be examined using the combination of *e*/*p* ratio and linear

Table 5 Cutting efficiency of ADC compared to traditional disc and pick cutting

Optimum cutting configuration		Specific energy, SE (MJ/m^3)		Cutting mechanism (uniaxial compressive strength of rock)	Reference
p^* (mm)	s^*/p or e/p	Laboratory	Numerical		
4	s/p = 10	41.70	43.10	Disc cutting (209 MPa)	Cho et al. (2013)
6	s/p = 10	37.60	40.50		
8	s/p = 7.5	35.00	37.80		
5	s/p = 4	67.57	41.05	Pick cutting (64 MPa)	Jeong et al. (2020a)
7	s/p = 3	42.17	40.99		
9	s/p = 3	33.12	42.08		
11	s/p = 3	31.10	43.10		
4	e/p = not defined (v = 20 mm/s)	< 20.51	-	Undercutting with ADC (206 MPa: scaled)	Present study
4	e/p = 1.4 (v = 30 mm/s)	33.86	-		
4	e/p = 1.4 (v = 40 mm/s)	50.49	-		
3	e/p = 1.875 (v = 20 mm/s)	20.51	-		
4	e/p = not defined (v = 30 mm/s)	< 44.84	-		
5	e/p = not defined (v = 40 mm/s)	< 43.85	-		

* The p and s are penetration depth and cut spacing, respectively

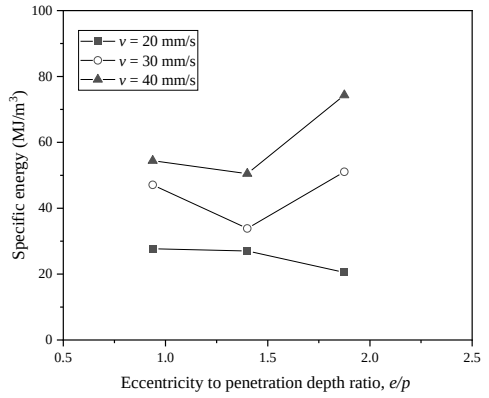

(a)

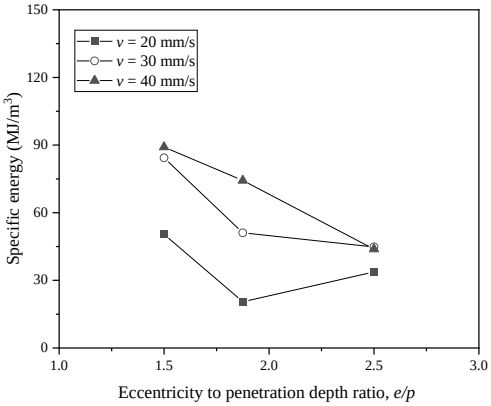

(b)

Fig. 17 Results of specific energy in various linear velocity and e/p ratio scenarios at (a) constant eccentricity (b) constant penetration depth

cutting velocity and potentially other cutting parameters such as rotational speed (RPM), diameter, and tilting angle of ADC.

Another important issue is how the ADC performs compared to traditional disc and pick cutting. Table 5 summarizes the optimum ADC cutting condition from the current investigation compared to conventional disc and pick cutting; Based on Cho *et al*. (2013) work, at the optimum condition, disc cutting yielded SE values in the range of 35-42 MJ/m^3 from the LCM test and 37-43 MJ/m^3 from numerical simulation. In the case of pick cutting, Jeong *et al.* (2020a) reported SE values ranging from 37 to 68 MJ/m^3 from the LCM test and 41 to 43 MJ/m^3 from numerical modeling; it is noted that the results of pick cutting are for medium-strength of rock. The use of conical pick usually is limited for the strength of rock up to 100 MPa. The optimal SE in the current study ranges from 20 MJ/m^3 to 50 MJ/m^3. Despite the fact that it is difficult to conclude whether ADC performs better or not compared to the standard cutting tools at the current research due to a lack of data, the results show a good indication, where the SE range can potentially drop to 20 MJ/m^3 using ADC. In addition, it should be noted that the results of ADC are obtained from the scaled test, not from the real scale. Future work using a more extensive database is necessary to confirm the current findings.

5. Conclusions

This study introduces the testing method and technique that enables evaluating cutting performance based on the undercutting method using an actuated disc cutter (ADC). In ADC, cutting force is determined by the resultant force and its orientation relative to the cutting direction. The

specific energy is estimated by the total work performed at the segmented length along the cutting trajectory. The commonly used *s*/*p* ratio cannot be used to determine the cutting efficiency of ADC since there is no interaction between adjacent cuts. Instead, the ratio of eccentricity and penetration depth (*e/p*) concept is proposed and tested using some cases in the laboratory. In the range of data presented in this paper, specific energy is affected by the *e/p* ratio and has optimal values in certain scenarios. Comparison with past research is made and it shows an indication that ADC is possibly more efficient than conventional disc and pick cutting by exhibiting a comparatively lower specific energy at its optimal cutting state. Further research is necessary to complement the current findings by extending the database and including other possible variables.

Acknowledgments

This study was funded by the Korea Agency for Infrastructure Technology Advancement under Ministry of Land, Infrastructure and Transport in Korea (Project No.: 20CTAP-C151926-02). This study was supported by the National Research Foundation of Korea (NRF) grant funded by the Korea government (MSIT) (No. NRF-2021R1G1A1091572).

References

Bilgin, N., Copur, H. and Balci, C. (2014), *Mechanical Excavation in Mining and Civil Industries*, CRC Press, Boca Raton, FL, USA.

Cho, J.W., Jeon, S., Jeong, H.Y. and Chang, S.H. (2013), "Evaluation of cutting efficiency during TBM disc cutter excavation within a Korean granitic rock using linear-cutting-machine testing and photogrammetric measurement", *Tunn. Undergr. Sp. Tech.*, **35**, 37-54. https://doi.org/10.1016/j.tust.2012.08.006.

Chang, S., Lee, C., Kang, T., Ha, T. and Choi, S. (2017), "Effect of hardfacing on wear reduction of pick cutters under mixed rock conditions", *Geomech. Eng.*, **13**(1), 141-159. https://doi.org/10.12989/gae.2017.13.1.141.

Copur, H., Bilgin, N., Balci, C., Tumac, D. and Avunduk, E. (2017), "Effects of different cutting patterns and experimental conditions on the performance of a conical drag tool", *Rock Mech. Rock Eng.*, **50**, 1585-1609. https://doi.org/10.1007/s00603-017-1172-8.

Dehkhoda, S. and Detournay, E. (2017), "Mechanics of actuated disc cutting", *Rock Mech. Rock Eng.*, **50**(2), 465-483. https://doi.org/10.1007/s00603-016-1121-y.

Dehkhoda, S. and Detournay, E. (2018), "Rock cutting with an actuated disc: an experimental study", *Proceedings of the 52nd U.S Rock mechanics/Geomechanics symposium*, Seattle, Washington. June.

Dehkhoda, S. and Detournay, E. (2019), "Rock cutting experiments with an actuated disc", *Rock Mech. Rock Eng.*, **52**(9), 3443-3458. https://doi.org/10.1007/s00603-019-01767-y.

Dehkhoda, S. and Hill, B. (2019), "Clearance angle and evolution of depth of cut in actuated disc cutting", *J. Rock Mech. Geotech. Eng.*, **11**(3), 644-658. https://doi.org/10.1016/j.jrmge.2018.12.010.

Hood, M. and Alehossein, H. (2000), "A development in rock cutting technology", *Int. J. Rock Mech. Min. Sci.*, **37**, 297-305. https://doi.org/10.1016/S1365-1609(99)00107-0.

Hood M. and Roxborough, F. (1992), *SME Mining Engineering Handbook*, (2nd Edition), Society of Mining, Metallurgy, and Exploration, Englewood, CO, USA.

Jeong, H., Cho, J., Jeon, S. and Rostami, J. (2016), "Performance assessment of hard rock TBM and rock boreability using punch penetration test", *Rock Mech. Rock Eng.*, **49**, 1517-1532. https://doi.org/10.1007/s00603-015-0834-7.

Jeong, H. and Jeon, S. (2018), "Characteristic of size distribution of rock chip produced by rock cutting with a pick cutter", *Geomech. Eng.*, **15**(3), 811-822. https://doi.org/10.12989/gae.2018.15.3.811.

Jeong, H., Choi, S., Lee, S. and Jeon, S. (2020a), "Rock cutting simulation of point attack picks using the smooth particle hydrodynamics technique and the cumulative damage model", *Appl. Sci.*, **10**, 5314. https://doi.org/10.3390/app10155314.

Jeong, H., Wicaksana, Y., Kim, S. and Jeon, S. (2020b), "Fundamental study on rock cutting by an actuated undercutting disc", *Tunn. Undergr. Sp.*, **30**(6), 592-602. https://doi.org/10.7474/TUS.2020.30.6.591.

Jeong, H., Choi, S. and Jeon, S. (2020c), "Effect of skew angle on the cutting performance and cutting stability of point-attack type picks", *Tunn. Undergr. Sp. Tech.*, **103**, 103507. https://doi.org/10.1016/j.tust.2020.103507.

Jeong, H., Wicaksana, Y., Kim, S. and Jeon, S. (2021), "Assessment of rock cutting efficiency of an actuated undercutting disc", *J. Korean Tunn Undergr Sp. Assoc.*, **23**(3), 199-209. https://doi.org/10.9711/KTAJ.2021.23.3.199.

Karekal, S. (2013), "Oscillating disc cutting technique for hard rock excavation", *Proceedings of 47th U.S. Rock Mechanics/Geomechanics Symposium, San Francisco, California, June.*

Kim, K., Jo, S., Ryu, H. and Cho, G. (2020), "Prediction of TBM performance based on specific energy", *Geomech. Eng.*, **22**(6), 489-496. https://doi.org/10.12989/gae.2020.22.6.489.

Kovalyshen, Y. (2015), "Analytical model of oscillatory disc cutting", *Int. J. of Rock Mech. Min. Sci.*, **77**, 378-383. https://doi.org/10.1016/j.ijrmms.2015.04.015.

Pan, Y., Liu, Q., Peng, X., Liu, Q., Liu, J., Huang, X., Cui, X. and Cai, T. (2019), "Full-scale linear cutting tests to propose some empirical formulas for TBM disc cutter performance prediction", *Rock Mech. Rock Eng.,* **52**, 4763-4783. https://doi.org/10.1007/s00603-019-01865-x.

Ramezanzadeh, A. and Hood, M. (2010), "A state-of-the-art review of mechanical rock excavation technologies", *Int. J. Min. Reclam. Environ.*, **1**(1), 29-39.

Xu, R. and Dehkhoda S. (2019), "Effect of actuation on rock fragmentation in undercutting discs", *Proceedings of the 53rd U.S. Rock Mechanics/Geomechanics Symposium,* New York, New York, June.

Xu, R., Dehkhoda, S., Hagan, P. and Oh, Y. (2021), "Evaluation of cutting fragments in relation to force dynamics in actuated disc cutting", *Int. J. Rock Mech. Min. Sci.*, **146**, 104850. https://doi.org/10.1016/j.ijrmms.2021.104850.

Zhu, X., Liu, W. and Lv, Y. (2017), "The investigation of rock cutting simulation based on discrete element method", *Geomech. Eng.*, **13**(6), 977-995. https://doi.org/10.12989/gae.2017.13.6.977.

Zhang, G., Dang, W., Herbst, M. and Song, Z. (2020), "Complex analysis of rock cutting with consideration of rock-tool interaction using distinct element method (DEM)", *Geomech. Eng.*, **20**(5), 421-432. https://doi.org/10.12989/gae.2020.20.5.421.